Structural degeneracy in pair distance distributions ᴇᴘ

Frank H. Stillinger 🆔, and Salvatore Torquato

COLLECTIONS

ᴇᴘ   This paper was selected as an Editor's Pick

View Online   Export Citation   CrossMark

ARTICLES YOU MAY BE INTERESTED IN

Structural degeneracy in pair distance distributions (EP)

View Online   Export Citation   CrossMark

Frank H. Stillinger[1,a)] (iD) and Salvatore Torquato[2,b)]

AFFILIATIONS

[1] Department of Chemistry, Princeton University, Princeton, New Jersey 08544, USA

[2] Department of Chemistry, Department of Physics, Princeton Institute for the Science and Technology of Materials, and Program in Applied and Computational Mathematics, Princeton University, Princeton, New Jersey 08544, USA

[a)] fhs@princeton.edu
[b)] torquato@electron.princeton.edu

ABSTRACT

A traditional basic descriptor of many-particle systems has been the distribution of interparticle pair distances. In the case of structureless particles at thermal equilibrium, with just additive pair interactions, this suffices to determine pressure and mean energy. However, it is usually the case that a given set of pair distances can emerge from a multiplicity of distinguishable many-particle configurations. This paper focuses on the ways in which such a configuration detail can be overlooked. After providing some elementary small-system examples in which full pair distance specification still permits distinct configurational pattern ambiguity, subsequent analysis concentrates on large-system classical canonical ensembles. In that context, configurational degeneracy is analyzed in two-dimensional systems for the shape distribution of triangles, whose chirality occurrence can be controlled by suitable three-particle interactions. For many-particle systems in three dimensions, the possibility is explored that a set of three-particle "pair-invisible" interactions can exist which modify the three-particle distribution function, but which have no effect on the pair distribution function, and thus remain undetected by conventional diffraction experiments. For illustration, a specific mathematical example is presented, applicable to the case where two-particle interactions vanish.

Published under license by AIP Publishing. https://doi.org/10.1063/1.5096894

I. INTRODUCTION

The instantaneous spatial configuration of a number N of identical structureless particles in d-dimensional Euclidean space R^d involves a set of $N(N-1)/2$ scalar pair distances. In general, this set is insufficient to determine uniquely the shape exhibited by the detailed configuration geometry of that N-particle set. But in certain circumstances, it can provide significant basic information. The many-body formalism of classical statistical mechanics presents well-known examples of such sufficiency: If the particles constitute a uniform fluid phase and interact just with spherically symmetric pair interactions, then under thermodynamic equilibrium conditions, the isotropic pressure and mean interaction energy depend geometrically only on the isotropic pair distribution function $\rho^{(2)}(r)$, i.e., the distribution of scalar distances.[1,2]

History presents an example in which the scalar pair distance distribution has been used frequently to supply an approximation

for the corresponding three-particle distribution function $\rho^{(3)}(r_{12}, r_{13}, r_{23})$. That example is the "Kirkwood superposition approximation."[3,4] Specifically, this assumes that the three-particle distribution function can be replaced by a suitably normalized product of pair distribution functions for each of the three particle pairs involved. In particular, this generates nonlinear integral equation approximations for the pair distribution functions that are amenable to numerical solution.[5]

The primary objective of the present investigation is to illustrate and examine the geometric uncertainties intrinsic to the scalar pair distance distribution when it is considered alone. This will first involve specific small-N cases to highlight the underlying basic problem, followed by analysis of large-N asymptotic-limit cases for well-defined equilibrium statistical ensembles.

As an appropriate starting point, Sec. II presents some elementary small-N examples for simple two- and three-dimensional particle configurations, explicitly exhibiting distinctively alternative

shapes with identical scalar distance sets. In preparation for analysis of the structural degeneracies that larger many-particle sets can exhibit, Sec. III recalls some preparatory statistical mechanical formalism for configuration ensembles. This is followed by Sec. IV in which it is emphasized that scalene triangles confined to two dimensions possess an intrinsic chirality, which automatically generates geometric ambiguity in an N-particle analysis based only on the pair distance distribution. A set of three-particle interactions is then introduced to exercise some control over that two-dimensional ambiguity.

Section V presents some general features of classical N-particle canonical equilibrium systems in three dimensions. Specifically, it considers the configurational distribution details resulting from coupling 3-particle interactions into systems initially subject only to 2-particle interactions. The underlying intention is ultimately to identify nontrivial "pair-invisible" 3-particle interactions that leave the system's pair distribution function unchanged. Section VI provides a clear circumstance for attaining that goal by assuming that the pair interactions vanish, i.e., the N-particle system is an ideal gas prior to coupling in the 3-particle interactions. Section VII provides a specific mathematical example of a vanishing influence of three-particle interactions upon the pair distance distribution, at least in the leading two orders of perturbation. The results presented in Secs. VI and VII are augmented by the Appendix suggesting a future numerical approach to the identification of three-particle interactions obeying the vanishing influence requirement on the pair distance distribution. Section VIII presents various discussion issues and conclusions.

II. SMALL-N ELEMENTARY EXAMPLES

A sensible starting point for the wider examination of the structural degeneracy problem involves full geometric description of some specific spatial patterns for a small number of points. Two cases will be described in detail, but many other examples can easily be created.

The first example consists of four points in two-dimensional Euclidean space. This has been previously described in a published paper[6] but provides a useful initial illustration for the present analysis. With an appropriate selection of the six pair distances, this involves geometric degeneracy between "kite" and "trapezoid" shapes that are illustrated in Fig. 1. Aside from overall expansion/contraction of the patterns (as well as the trivial possibilities of pattern translation and rotation), there is an additional parameter choice $1/2 < x < 1$ that controls the specific shapes of the "kite" and "trapezoid" alternatives. The scalar lengths shown in Fig. 1 have the following x-dependent magnitudes:

$$a(x) = (2x^2 - 3x + 5/4)^{1/2},$$
$$b(x) = (2x^2 - x + 1/4)^{1/2},$$
$$c(x) = 2x - 1,$$
$$d(x) = 1.$$
(1)

It should be noted in passing that if one were to choose $x > 1$, the outer boundary of the "kite" pattern would become an isosceles triangle, but its structural degeneracy property with the trapezoid would persist.
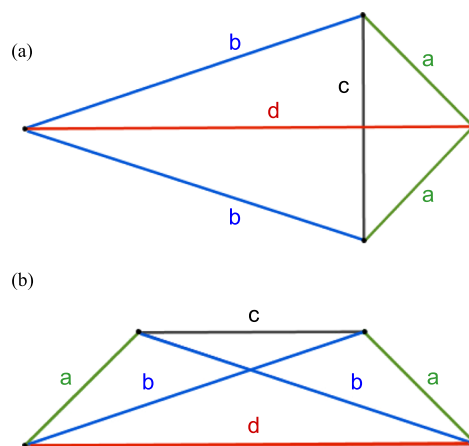

FIG. 1. The (a) "kite" and (b) "trapezoid" geometrically degenerate configuration pair for four points in two dimensions.[6] The six scalar pair distances adopt four interrelated values $a(x)$, $b(x)$, $c(x)$, $d(x)$ specified in Eq. (1).

A second example again involves four points but now inhabiting three-dimensional Euclidean space. The six pair distances are restricted so as to possess only two magnitudes: three have a short distance s and the other three have a longer distance l, subject to the constraints,

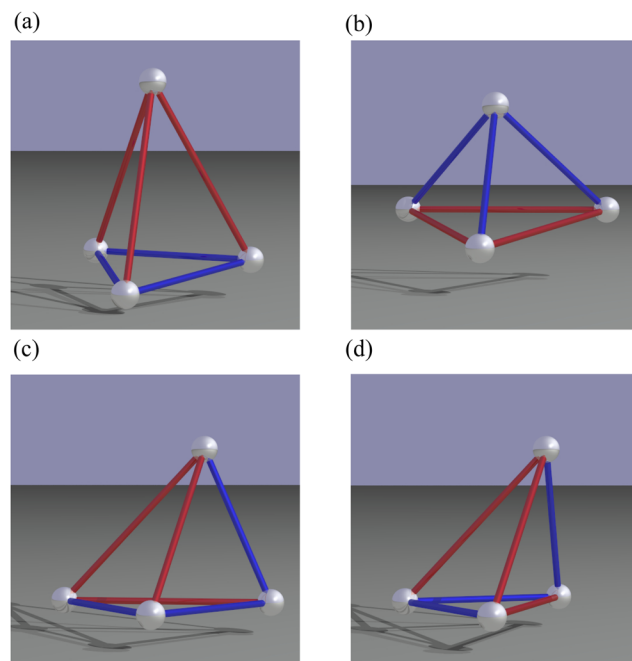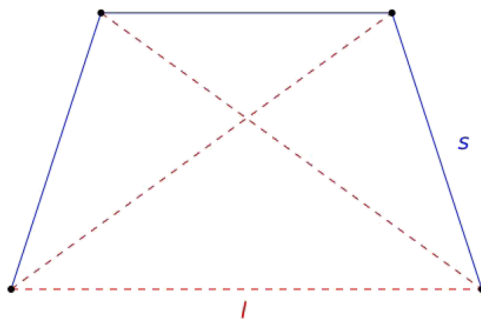$$0 < s < l < [(5^{1/2} + 1)/2]s.$$
(2)

FIG. 2. Distinct tetrahedra that can be constructed from three short pair distances s (blue lines) and three larger pair distances l (red lines) subject to the constraints in Eq. (2).

FIG. 3. Planar achiral pattern adopted jointly by the tetrahedra shown in Fig. 2(c) and 2(d) as the distance ratio $l/s \rightarrow (5^{1/2} + 1)/2$, the "golden ratio."

These pair distances can be arranged into four distinct tetrahedral shapes, illustrated graphically in Fig. 2. Two of these tetrahedra, Figs. 2(a) and 2(b), possess reflection and rotation symmetries. The other two, Figs. 2(c) and 2(d), are asymmetric but constitute mirror images of each other. Note that the upper limit imposed on l represents the collapse of the chiral patterns 2(c) and 2(d) to a common planar nonchiral pattern, illustrated in Fig. 3.

Reference 6 provides additional examples of structural degeneracy in two and three dimensions, including cases with more than four point particles ($N > 4$). Furthermore, structural degeneracy situations have also been identified for the $N \rightarrow +\infty$ limit, where the point collections constitute a continuous phase pattern in a heterogeneous two-phase region.[7]

III. STATISTICAL MECHANICAL FORMALISM

The general issue of structural degeneracy underlying the distribution of scalar distances is also relevant to selected cases of configurational ensembles. For the present analysis, attention will now be focused on canonical ensembles of $N \geq 3$ identical point particles in a fixed d-dimensional volume V, at temperature $T > 0$. The volume V will be simply connected and will be required to have a shape exhibiting a reflection symmetry, i.e., the shape of V is achiral. It will also be assumed that V possesses rigid boundaries that are particle-impenetrable but that otherwise are noninteracting with the contained particles. This section will present some relevant definitions and relations for such canonical ensembles.

The N particles at positions $\mathbf{r}_1 \cdots \mathbf{r}_N$ within V will be presumed to experience a potential energy function $\Phi(\mathbf{r}_1 \cdots \mathbf{r}_N)$ that is bounded below and fully symmetric with respect to particle location exchanges. The classical canonical partition function then has the form[8]

$$Q_N(T, V) = (\lambda_T{}^{dN} N!)^{-1} Z_N(T, V),$$
$$Z_N(T, V) = \int_V d\mathbf{r}_1 \cdots \int_V d\mathbf{r}_N \exp[-\Phi(\mathbf{r}_1 \cdots \mathbf{r}_N)/k_B T]. \quad (3)$$

Here, k_B is Boltzmann's constant, λ_T stands for the mean thermal de Broglie wavelength of the particles, assumed to have mass m, and h is Planck's constant

$$\lambda_T = \frac{h}{(2\pi m k_B T)^{1/2}}. \quad (4)$$

Density distribution functions $\rho^{(n)}(\mathbf{r}_1 \cdots \mathbf{r}_n)$, for n particles, $1 \leq n \leq N$, in this canonical ensemble are defined by

$$\rho^{(n)}(\mathbf{r}_1 \cdots \mathbf{r}_n) = \left[\frac{N!}{(N - n)! Z_N} \right] \int_V d\mathbf{r}_{n+1} \cdots \int_V d\mathbf{r}_N$$
$$\times \exp[-\Phi(\mathbf{r}_1 \cdots \mathbf{r}_N)/k_B T]. \quad (5)$$

These functions provide the simultaneous occurrence probability of any n particles in incremental volumes located at the positions $\mathbf{r}_1 \cdots \mathbf{r}_n$.[2] The pair distribution function $\rho^{(2)}(\mathbf{r}_1, \mathbf{r}_2)$ for given values of N, T, and V contains sufficient information to allow extraction of $P(r)$, the ensemble average distribution of scalar pair distances,

$$P(r) = (1/2) \int_V d\mathbf{r}_1 \int_V d\mathbf{r}_2 \delta(r - |\mathbf{r}_1 - \mathbf{r}_2|) \rho^{(2)}(\mathbf{r}_1, \mathbf{r}_2), \quad (6)$$

where $\delta(\cdots)$ is the Dirac delta function. If $R_{\max}$ represents the largest scalar distance that fits inside V, then

$$\int_0^{R_{\max}} P(r) dr = N(N - 1)/2. \quad (7)$$

For present purposes, it will suffice to restrict the N-particle potential energy function just to pair and triplet interactions

$$\Phi(\mathbf{r}_1 \cdots \mathbf{r}_N) = \sum_{i=2}^{N} \sum_{j=1}^{i-1} \varphi_2(r_{ij}) + \sum_{i=3}^{N} \sum_{j=2}^{i-1} \sum_{k=1}^{j-1} \varphi_3(\mathbf{r}_i, \mathbf{r}_j, \mathbf{r}_k). \quad (8)$$

The functions φ_2 and φ_3 are each constrained to be invariant to translation and proper rotation of the particle pair or triplet geometry involved. One of the primary interests in Secs. IV–VII concerns how the scalar pair distribution $P(r)$ would change (if at all), starting just with the collection of pair interactions φ_2 and then continuously coupling in the three-body interactions φ_3.

IV. TRIANGLE CHIRALITY IN TWO DIMENSIONS

The lack of symmetry for scalene triangles implies that each one possesses three unequal side lengths. For $d = 2$, this creates the existence of chiral pairs of scalene triangles, a typical example of which is illustrated in Fig. 4. Such triangles can be classified by the rotational direction around which the side-length sequence must proceed in the short-medium-long order, the two possibilities of which are simply "clockwise" and "anticlockwise." If the N-particle system's potential energy function Φ contains only isotropic pair interactions $\varphi_2(r_{ij})$, then the canonical ensemble configurational probability inside a $d = 2$ symmetric container shape V, proportional to the Boltzmann factor $\exp(-\Phi/k_B T)$, necessarily assigns equal probabilities to the clockwise and the counterclockwise versions of all triangle mirror-image pairs. However, for this $d = 2$ situation, appropriately chosen triplet interactions $\varphi_3(\mathbf{r}_i, \mathbf{r}_j, \mathbf{r}_k)$ can upset that probability equality.

A passing comment about the 4-point, 6-distance degeneracy examples displayed in Fig. 1 may be useful. The "kite" shape,
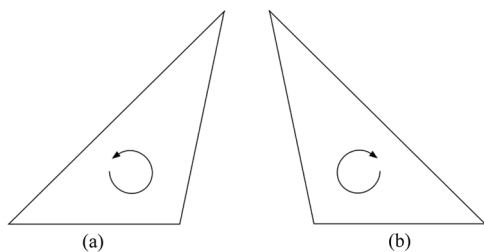
FIG. 4. Two scalene triangles that are a mirror-image (chiral) pair in two dimensions ($d = 2$). The internal arrow rotation directions are determined by the ordering of the sides: short-middle-long: (a) counterclockwise rotation and (b) clockwise rotation.

Fig. 1(a), contains two isosceles triangles and a mirror-image pair of chiral scalene triangles. The "trapezoid" shape, Fig. 1(b), contains two distinct pairs of mirror-image chiral scalene triangles. The "kite" and "trapezoid" shapes each possess reflection symmetries and are therefore achiral.

In this two-dimensional scenario, define a function $\chi(\mathbf{r}_i, \mathbf{r}_j, \mathbf{r}_k)$ to be a chirality identifier for a triangle formed by particles i, j, and k,

$$\chi(\mathbf{r}_i, \mathbf{r}_j, \mathbf{r}_k) = -1 \quad \text{(counterclockwise rotation shape)}$$
$$= 0 \quad \text{(isosceles, equilateral, or vanishing area shapes)}$$
$$= +1 \quad \text{(clockwise rotation shape)}. \quad (9)$$

One should note that χ can be computed by augmenting the $d = 2$ Euclidean space with a third dimension and then observing the sign of a vector cross product from a directed pair of triangle side displacements consistent with the assigned short-medium-long sequence directional ordering.

Then, consider the following family of three-particle interaction functions:

$$\varphi_3(\mathbf{r}_i, \mathbf{r}_j, \mathbf{r}_k) = \xi q(r_{ij}, r_{ik}, r_{jk})\chi(\mathbf{r}_i, \mathbf{r}_j, \mathbf{r}_k); \quad (10)$$

here, the spatial function q is chosen to be symmetric with respect to all permutations of its three scalar distance variables. In particular, the function q may be chosen to vanish if any of its three distance variables exceed a selected length L, $0 < L < R_{max}$, but will otherwise be required to satisfy $q > 0$. Equation (10) also includes a coupling parameter $|\xi| \geq 0$ that can be used to continuously turn on the triplet interactions within the N-particle system.

By employing the chirality identifier χ, it is possible to evaluate the numbers of clockwise (C_+) and counterclockwise (C_-) triangles present in any N-particle configuration. The corresponding canonical ensemble averages then satisfy

$$\langle C_+ \rangle + \langle C_- \rangle = N(N-1)(N-2)/3!, \quad (11)$$

after acknowledging that $\chi = 0$ cases normally have vanishing probability. In the absence of three-particle interactions such as shown in Eq. (10), the ensemble averages as noted earlier must assign equal probabilities to clockwise and anticlockwise occurrences

$$\langle C_+ \rangle - \langle C_- \rangle = 0 \quad (\xi = 0). \quad (12)$$

Now consider the effect of imposing a small deviation from the origin of coupling constant ξ. If $\xi > 0$, the statistical effect of the 3-particle interactions specified in Eq. (10) would be to reduce $\langle C_+ \rangle$ while increasing $\langle C_- \rangle$ by a corresponding amount to maintain the validity of Eq. (11). This leading-order influence would be a perturbation linear in the coupling parameter ξ,

$$\langle C_+ \rangle - \langle C_- \rangle = O(\xi) < 0, \quad (13)$$

and in this leading order should only influence those triangles for which $q > 0$, i.e., triangles with all three $r_{ij} \leq L$. However, it needs to be stressed that the pair distance distribution function $P(r)$, Eq. (6), will not exhibit a corresponding modification that is linear in ξ.

A primary conclusion to be drawn from this elementary analysis is that the Kirkwood superposition approximation[3,4] is obviously incapable of describing any chiral bias among triangles in $d = 2$ that had been imposed on the canonical triangle distribution function represented by $\rho^{(3)}(\mathbf{r}_1, \mathbf{r}_2, \mathbf{r}_3)$. Application of the superposition approximation to the three-particle configuration distribution inevitably leads to $\langle C_+ \rangle = \langle C_- \rangle$.

If the coupling strength parameter ξ were to increase in magnitude beyond the weak linear regime, the scalar distance distribution $P(r)$ and the net chirality measure $\langle C_+ \rangle - \langle C_- \rangle$ could develop $O(\xi^2)$ and higher order "corrections." However, these nonlinear effects could be neutralized by supplementing the three-particle interaction form shown in Eq. (10) with additional three-particle interactions that are themselves higher order in ξ than linear. It should be kept in mind that the spatial range of these additional φ_3 components might have to exceed L.

V. THREE-DIMENSIONAL ANALYSIS

Upon increasing the Euclidean space dimension d from 2 to 3, the triangle chirality concept specified by χ, Eq. (9), is no longer relevant. However, there are other measures that can be used in three dimensions to distinguish and classify triangle shapes. One straightforward example is the dimensionless ratio of a triangle's area A to the square of its perimeter

$$\eta(r, s, t) = A(r, s, t)/(r + s + t)^2, \quad (14)$$

where temporarily the three triangle side lengths have been denoted just by r, s, and t. This specific triangle shape measure lies in the range

$$0 \leq \eta \leq (12 \cdot 3^{1/2})^{-1}, \quad (15)$$

where the upper limit corresponds to equilateral triangle shape ($r = s = t$). Any deviation from that equilateral shape causes η to decrease, finally vanishing when the triangle degenerates to a zero-area single line interval.

In order to maintain connection with the results of Sec. IV, attention now will be focused on the possible existence in $d = 3$ of three-particle interactions φ_3 that at given particle density and temperature will perturb triangle distributions while leaving the pair

distance distribution unchanged. For notational simplicity, set

$$\Phi^{(2)}(\mathbf{r}_1\cdots\mathbf{r}_N) = \sum_{i=2}^{N}\sum_{j=1}^{i-1}\varphi_2(r_{ij}), \tag{16}$$

$$\Phi^{(3)}(\mathbf{r}_1\cdots\mathbf{r}_N) = \sum_{i=3}^{N}\sum_{j=2}^{i-1}\sum_{k=1}^{j-1}\varphi_3(r_{ij}, r_{ik}, r_{jk}). \tag{17}$$

Note that the irrelevancy of triangle chirality as d has been increased from 2 to 3 implies that each three-particle interaction function φ_3 in Eq. (17) is now just a function of the three scalar edge distances, not their vectors as in the prior equations (8) and (10). With these abbreviated notations, the formal expression for the canonical ensemble's nth order distribution function from Eqs. (3) and (5) can be trivially rewritten as follows ($\beta = 1/k_B T$):

$$\rho^{(n)}(\mathbf{r}_1\cdots\mathbf{r}_n) = \left[\frac{N!}{(N-n)! Z_N}\right]\int_V d\mathbf{r}_{n+1}\cdots\int_V d\mathbf{r}_N$$
$$\times \exp\left[-\beta\left(\Phi^{(2)} + \Phi^{(3)}\right)\right], \tag{18}$$
$$Z_N = \int_V d\mathbf{r}_1\cdots\int_V d\mathbf{r}_N \exp\left[-\beta\left(\Phi^{(2)} + \Phi^{(3)}\right)\right].$$

At this stage, it is useful to invoke a three-particle interaction generalization of the Mayer cluster expansion that was originally developed for gas-phase virial series.[9] The Boltzmann factor appearing in Eqs. (18) for the three-particle interactions is thus expanded in the following way:

$$\exp\left[-\beta\Phi^{(3)}(\mathbf{r}_1\cdots\mathbf{r}_N)\right] = \prod_{1\le i<j<k}^{N}\left[1 + f_3(r_{ij}, r_{ik}, r_{jk})\right], \tag{19}$$

where

$$f_3(r_{ij}, r_{ik}, r_{jk}) = \exp\left[-\beta\varphi_3(r_{ij}, r_{ik}, r_{jk})\right] - 1 \ge -1. \tag{20}$$

The resulting generalized Mayer cluster expansion is useful if the triplet interactions φ_3 (and therefore the corresponding f_3) are weak and/or if they are short ranged compared to the $d = 3$ neighbor-average particle separation measure $(V/N)^{1/3}$. Equations (18) and (19) then can serve as the starting points for distribution function series whose terms involve increasing order of the f_3 effects; formally, this can be expressed as follows:

$$\rho^{(n)}(\mathbf{r}_1\cdots\mathbf{r}_n) = \sum_{l=0}^{N}\rho^{(n,l)}(\mathbf{r}_1\cdots\mathbf{r}_n). \tag{21}$$

Here, $\rho^{(n,0)}$ is the n-particle distribution function in the absence of triplet interactions $\Phi^{(3)}$, $\rho^{(n,1)}$ represents the leading (linear) order correction due to weak triplet perturbation, and subsequent terms systematically present the development of higher order modifications (quadratic, cubic, quartic, . . .) due to increasing influence of the triplet interactions via the f_3.

Figure 5 provides a schematic diagram of the various f_3 terms that are generated upon carrying out the product indicated by the right member of Eq. (19). The individual f_3's are represented by triangles, the vertices of which correspond to individual particle locations. The figure illustrates the fact that the generated terms amount to connected clusters that result from distinct f_3 triangles sharing
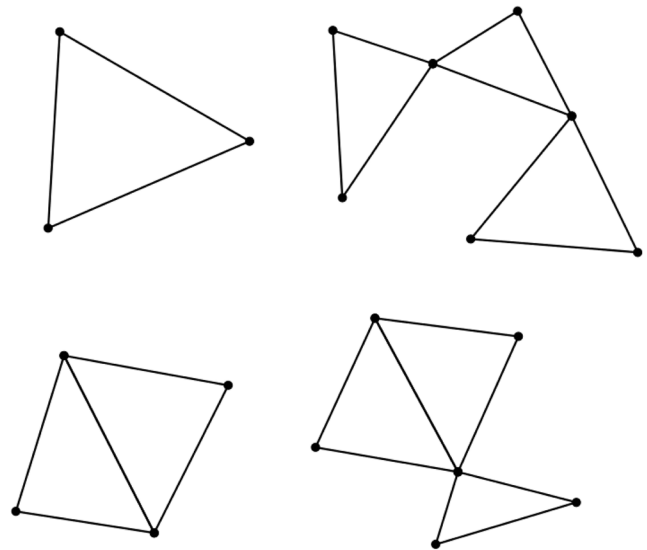

FIG. 5. Schematic diagram of the types of terms that arise from the expansion of the right member of Eq. (19). Individual f_3 factors are represented by triangles, the vertices of which are particle positions. Connected clusters of triangles arise from sharing of one or two vertices.

one or two vertices (particle positions). This characteristic of the terms produced by the expansion of Eq. (19) will be directly relevant in Sec. VI.

Using Eqs. (18) and (19), the linear correction term for the pair correlation function is found to have the following detailed format:

$$\rho^{(2,1)}(\mathbf{r}_1, \mathbf{r}_2) = \int_V d\mathbf{r}_3 \rho^{(3,0)}(\mathbf{r}_1, \mathbf{r}_2, \mathbf{r}_3) f_3(r_{12}, r_{13}, r_{23})$$
$$+ \frac{1}{2}\int_V d\mathbf{r}_3\int_V d\mathbf{r}_4 \rho^{(4,0)}(\mathbf{r}_1, \mathbf{r}_2, \mathbf{r}_3, \mathbf{r}_4)$$
$$\times \left[f_3(r_{13}, r_{14}, r_{34}) + f_3(r_{23}, r_{24}, r_{34})\right]$$
$$+ \frac{1}{6}\int_V d\mathbf{r}_3\int_V d\mathbf{r}_4\int_V d\mathbf{r}_5\Big[\rho^{(5,0)}(\mathbf{r}_1, \mathbf{r}_2, \mathbf{r}_3, \mathbf{r}_4, \mathbf{r}_5)$$
$$- \rho^{(2,0)}(\mathbf{r}_1, \mathbf{r}_2)\rho^{(3,0)}(\mathbf{r}_3, \mathbf{r}_4, \mathbf{r}_5)\Big]f_3(r_{34}, r_{35}, r_{45}). \tag{22}$$

In principle, this result is applicable to cases where the unperturbed starting point ($\Phi^{(3)} = 0$) could involve either vapor, liquid, or crystalline phases. The last of these would possess distribution functions $\rho^{(n,0)}$ exhibiting long-range periodic and orientational order. If Eq. (22) is to be used to identify nonvanishing f_3 functions (i.e., nonvanishing φ_3 interactions) for which the linear response function $\rho^{(2,1)}$ vanishes identically, it is clear that the results would be sensitive to the starting thermodynamic phase involved through its characteristic distribution function details.

VI. PERTURBED IDEAL GAS

For the present exploratory analysis, attention will be focused on the elementary case with $\Phi^{(2)} \equiv 0$, that is, the N-particle

canonical ensemble acting as a classical ideal gas before including coupling via the triplet interactions $\Phi^{(3)}$. The basic issue then is whether any triplet interactions can be identified whose effects at least in linear order will change $\rho^{(3)}$, while leaving $\rho^{(2)}$ unchanged. In this case, for the infinite-system limit with number density $\rho = N/V$, one has the obvious simplification ($n \geq 1$)

$$\rho^{(n,0)} \to \rho^n. \tag{23}$$

As a result, the general expression [Eq. (22)] reduces to the following equation:

$$
\begin{aligned}
\rho^{(2,1)}(r_{12}) &= \rho^3 \int d\mathbf{r}_3 f_3(r_{12}, r_{13}, r_{23}) + \frac{1}{2}\rho^4 \int d\mathbf{r}_3 \\
&\quad \times \int d\mathbf{r}_4 [f_3(r_{13}, r_{14}, r_{34}) + f_3(r_{23}, r_{24}, r_{34})] \\
&= \rho^3 \int d\mathbf{r}_3 f_3(r_{12}, r_{13}, r_{23}) + \rho^4 \int d\mathbf{r}_3 \int d\mathbf{r}_4 f_3(r_{13}, r_{14}, r_{34}).
\end{aligned}
\tag{24}
$$

A sufficient f_3 condition to cause this last $\rho^{(2,1)}$ expression (24) to vanish identically for any $r_{12} \geq 0$ is

$$\int d\mathbf{r}_3 f_3(r_{12}, r_{13}, r_{23}) = 0. \tag{25}$$

Consequently, any nonzero f_3 candidate must vary in sign in such a way that with two of its triangle vertices held fixed, the spatial integral over the third vertex position vanishes identically. Of course, such sign variation must be consistent with the permutation symmetry of the three vertex locations, and because f_3 is a symmetric function of three scalar distances, whereas this last condition is just a "one-dimensional" constraint, one should expect that a nontrivial family of functions that obey Eq. (25) exists.

The intrinsic linearity of condition (25) implies that if it is satisfied by a triplet function f_3, then so too will it be satisfied by a real multiple λf_3, provided it continues to obey the inequality shown in Eq. (20). Note also that if a triplet interaction φ_3 is identified for which Eq. (25) is satisfied at some specific temperature, a change in temperature will no longer permit that condition formally to be satisfied, but obviously a correspondingly energy-rescaled φ_3 would satisfy condition (25).

For the φ_3-perturbed ideal gas under consideration, with constraint equation (25) applied, one finds that the nonvanishing linear change in the triplet distribution function $\rho^{(3)}$ due to f_3 is simply

$$\rho^{(3,1)}(\mathbf{r}_i, \mathbf{r}_j, \mathbf{r}_k) = \rho^3 f_3(r_{ij}, r_{ik}, r_{jk}). \tag{26}$$

It is also important to note that the f_3 constraint equation (25) has a basic simplifying effect on the quadratic perturbation $\rho^{(3,2)}$ due to the fact that clusters comprised of two connected triangles inevitably have two or four unshared vertices, as illustrated in Figure 5. Integration over such unshared vertex positions automatically produces a vanishing result. Because this is the outcome for each of the contributions to the formal quadratic influence, one concludes that

$$\rho^{(3,2)}(\mathbf{r}_{ij}, \mathbf{r}_{ik}, \mathbf{r}_{jk}) \equiv 0. \tag{27}$$

However, the higher order results $\rho^{(3,l)}$ for $l \geq 3$ include nonvanishing contributions from triangle clusters that contain only shared vertices and so may not vanish.

VII. ILLUSTRATIVE EXAMPLE

In order to establish that the set of solutions to Eq. (25) is not empty, it suffices to exhibit at least one example. For notational simplicity, set

$$(r_{12}, r_{13}, r_{23}) \equiv (r, s, t). \tag{28}$$

Then, the illustrative example has the following form:

$$f_3(r, s, t) = F_0(r)\delta(r - s)\delta(r - t) - F_1(r)F_1(s)F_1(t), \tag{29}$$

where one must require

$$F_0(r) \geq 0 \tag{30}$$

in order to satisfy inequality (20).

Upon inserting the f_3 expression (29) into the integral requirement (25), one obtains

$$0 = 2\pi r F_0(r) - \frac{F_1(r)}{2\pi^2 r} \int_0^\infty dk\, k \sin(rk) H^2(k). \tag{31}$$

Here, $H(k)$ is the Fourier transform of the function F_1,

$$H(k) = \frac{4\pi}{k} \int_0^\infty du\, u \sin(ku) F_1(u). \tag{32}$$

Consequently, $F_0(r)$ would be determined by the choice of the radial function $F_1(u)$.

In the interest of providing an explicit example, consider the choice

$$F_1(u) = C \exp(-\alpha u^2), \tag{33}$$

where C and α are positive constants. Consequently, one has

$$H(k) = C\left(\frac{\pi}{\alpha}\right)^{3/2} \exp\left(-\frac{k^2}{4\alpha}\right). \tag{34}$$

Equation (31) then leads to the following result:

$$F_0(r) = \left(\frac{\pi^{1/2} C^3}{2^{5/2} \alpha^{3/2} r}\right) \exp\left(-\frac{3\alpha r^2}{2}\right), \tag{35}$$

thus completing determination of a solution for integral constraint equation (25).

Obviously, it would be desirable eventually to construct alternative solutions to Eq. (25). In particular, the occurrence of Dirac delta functions in the f_3 form (29) does not conform to conventional physical expectations for particle interactions. Instead, one would like to identify f_3 solutions that are bounded above and continuous. A possibly useful strategy to identify alternative f_3 solutions to integral equation (25), based upon a temporary discretization representation, appears in the Appendix.

VIII. DISCUSSION AND CONCLUSIONS

Beyond its historical relevance to the previously mentioned Kirkwood superposition approximation,[3,4] it is also worth noting a pedagogic connection of the present investigation to the "Reverse Monte Carlo Approach."[10] This latter method involves numerical identification of effective pair potentials $\Phi_{eff}^{(2)}$ that alone generate many-particle simulations whose results closely reproduce measured pair distribution functions (scalar pair distance distributions) for a condensed matter system of interest. Not surprisingly, the identified effective pair potentials depend on the initial system's temperature and pressure. Assuming that indeed classical statistical mechanics applies accurately, this reverse Monte Carlo approach intrinsically glosses over three-body, four-body, ..., interactions that may be present in the initial system of interest. A possibly useful extension of the reverse Monte Carlo approach would be to identify at least a three-body effective perturbation that, upon inclusion with a $\Phi_{eff}^{(2)}$ in simulations, could have a negligible effect on the pair correlation function at one temperature of interest but would reduce deviations of the reverse Monte Carlo pair distribution function results for other thermodynamic states of the many-particle system of interest.

Although there may be a set of "pair-invisible" three-particle interactions φ_3 for a many-particle system at given density and temperature, there certainly exist other system properties for which those interactions could produce "visible" effects. One such case concerns the adsorption behavior of a fluid phase on a structurally well-defined solid substrate surface. That surface often might present localized adsorption sites for the fluid's particles, geometrically arranged into specific triangular shape patterns. As stressed earlier, the three-particle interactions within the fluid phase have the effect of reducing the pair distance degeneracy by controlling the distribution of particle triangle sizes and shapes. Depending on the specific φ_3 form, this could either enhance or inhibit the presence of trimers available for fitting into those triangular adsorption site geometries, with corresponding influence on the solid-fluid interfacial free energy. Detailed analysis of the presence and magnitude of such adsorption phenomena qualifies for subsequent research examination.

It is worth noting that, if instead of the triplet interactions $\Phi^{(3)}$ analyzed in Sec. V for $d = 3$, one were to consider a permutation-symmetric set of quadruplet interactions $\Phi^{(4)}$, then it would be possible to bias the canonical distribution with respect to the chirality of tetrahedral particle patterns, such as those illustrated earlier in Figs. 2(c) and 2(d). Obviously, with only the pair interactions $\Phi^{(2)}$ present, the canonical distribution necessarily assigns equal probability to left and right handed tetrahedron structures. However, detailed examination of this $\Phi^{(4)}$ extension and its role in chirality symmetry breaking will need to await a future research project.

One intriguing possibility for such future research would be to create an explicit three-dimensional analog of the two-dimensional chirality identifier χ [Eq. (9)]. This analog would presumably separate the full configuration space for tetrahedra into a pair of simply connected subsets with respective identifier values ± 1, subject to a dividing interface that includes all achiral (mirror-symmetric) tetrahedron configurations with identifier value 0. An implication of such a definition is that any two tetrahedra with the same identifier value can be connected configurationally by a continuous deformation path along which the identifier remains constant.

APPENDIX: NUMERICAL APPROXIMATION

For the purposes of this proposed approach to the $d = 3$ problem, assume that $f_3(r, s, t)$ vanishes if any one of the three distances exceeds $0 < L < R_{max}$. That is, relevant values of f_3 are contained within the $L \times L \times L$ cube in r, s, t space

$$0 \leq r, s, t \leq L. \tag{A1}$$

This overall cube then will be divided into n^3 equivalent small cubes, where n is a positive odd integer. Thus, each of the distances r, s, and t will be equally divided into intervals of length $L/n \equiv \delta$. By introducing enumeration indices $1 \leq j, k, l \leq n$, the centers of these small cubes will thus be located at

$$r = (j - 1/2)\delta, \quad s = (k - 1/2)\delta, \quad t = (l - 1/2)\delta. \tag{A2}$$

The intention is to use the discrete set of values of f_3 at the small-cube centers to construct approximate solutions to integral equation (25). Not all of the n^3 centers are relevant; in particular, those cubes whose three center coordinates r, s, t violate the triangle inequality must be eliminated. Furthermore, among those cubes remaining after triangle-inequality elimination, those whose

TABLE I. List of relevant cube center locations for $n = 5$, subject to permutation-symmetry elimination constraints [Eq. (A3)]. The integer sets j, k, l determine the r, s, t coordinate values via Eq. (A2).

j	k	l	j	k	l
1	1	1	5	3	2
2	1	1	5	3	3
2	2	1	5	4	1
2	2	2	5	4	2
3	2	1	5	4	3
3	2	2	5	4	4
3	3	1	5	5	1
3	3	2	5	5	2
3	3	3	5	5	3
4	2	2	5	5	4
4	3	1	5	5	5
4	3	2			
4	3	3			
4	4	1			
4	4	2			
4	4	3			
4	4	4			

center coordinates differ only by r, s, t permutations (i.e., j, k, l permutations) must have identical f_3 value assignments. As an example, Table I presents the 28 distinct independent cube-center locations for $n = 5$, namely, those that do not violate the triangle inequality and that do not differ only by coordinate permutation. The specific choices shown conform to the permutation-avoiding convention

$$n \geq j \geq k \geq l \geq 1. \tag{A3}$$

For arbitrary choice of the positive odd integer n, one finds that the number of such independent cubes is given by the following cubic polynomial:

$$p(n) = (1/24)(2n^3 + 15n^2 + 10n - 3). \tag{A4}$$

The discrete sum approximation to the integral equation (25) appears as follows (r held fixed):

$$0 = \int d\mathbf{r}_3 f_3(r, s, t) \cong [2\pi\delta^3/r(j)] \sum_{k,l}^* s(k)t(l)f_3(j, k, l), \tag{A5}$$

where the asterisk on the summation indicates inclusion of all relevant cubes, including those with permuted indices k and l, with j fixed. There are n conditions of the type shown in the last line of Eq. (A5), one for each fixed j value. However, this must be viewed in the context of the cubic polynomial equation (A4), demonstrating that as n increases the number of unknown f_3 values assigned to cube centers far exceeds the number of constraints. By itself, this implies the existence of a large set of solutions. Of course, one is ultimately interested in the $n \to +\infty$ continuum limit, for which continuous f_3 functions would be desirable results.

It would be informative to try to obtain relatively simple f_3 solutions, starting with a reasonable approximation for the cube-center values and then adjusting those assigned values stepwise to reduce a mean-square error measure. One such pattern might be based on the triangle measure shown earlier in Eq. (14). Specifically, as an initial approximation, one could try

$$f_3(r, s, t) \propto \eta(r, s, t) - \eta_0, \tag{A6}$$

where η_0 is a positive constant present to provide a necessary sign change pattern.

REFERENCES

[1] T. L. Hill, in *Statistical Mechanics* (McGraw-Hill Book Co., New York, 1956), Chap. 6.

[2] J. P. Hansen and I. R. McDonald, in *Theory of Simple Liquids* (Academic Press, London, 1976), Chap. 2.

[3] J. G. Kirkwood, J. Chem. Phys. **3**, 300 (1935).

[4] J. G. Kirkwood and E. M. Boggs, J. Chem. Phys. **10**, 394 (1942).

[5] Reference 2, Sec. 5.4.

[6] Y. Jiao, F. H. Stillinger, and S. Torquato, Phys. Rev. E **81**, 011105 (2010).

[7] Y. Jiao, F. H. Stillinger, and S. Torquato, Phys. Rev. E **82**, 011106 (2010).

[8] Reference 2, p. 24.

[9] J. E. Mayer and M. G. Mayer, in *Statistical Mechanics* (John Wiley & Sons, New York, 1940), Chap. 13.

[10] A. P. Lyubartsev and A. Laaksonen, Phys. Rev. E **52**, 3730 (1995).